

Neural Network-Based Identification and Approximate Predictive Control of a Servo-Hydraulic Vehicle Suspension System

Olurotimi A. Dahunsi and Jimoh O. Pedro *

Abstract— This paper presents multi-layer feed-forward neural network-based identification and approximate predictive controller (NNAPC) for a two degree-of-freedom (DOF), quarter-car servo-hydraulic vehicle suspension system. The nonlinear dynamics of the servo-hydraulic actuator is incorporated in the suspension model. A suspension travel controller is developed to improve the ride comfort and handling quality of the system. A SISO neural network (NN) model based on Nonlinear AutoRegressive with eXogenous input (NARX) is developed using input-output data sets obtained from mathematical model simulation. The NN model was trained using Levenberg-Marquardt algorithm. The NNAPC was used to predict the future responses that are optimized by cost minimization. The proposed controller is compared with a constant-gain PID controller (based on Ziegler-Nichols tuning method) during suspension travel setpoint tracking in the presence of deterministic road disturbance. Simulation results demonstrate the superior performance of the NNAPC over the generic PID - controller in adapting to the deterministic road disturbance.

Keywords: Neural Networks, Model Predictive Control, PID Control, Ride Comfort, Suspension System, Servo-hydraulics, Handling Quality.

1 Introduction

Research interest in active vehicle suspension system has continued to grow since the late 1960s as progress was made in random vibrations research and optimal control theory [1, 2]. This development and the current rapid advances in electronics and intelligent control are enhancing the development of better active vehicle suspension system (AVSS). AVSS application holds good prospect despite drawbacks such as : higher cost; inherent system nonlinearities and uncertainties; hardware complexity; actuator dynamics complications; and varying oper-

ating conditions of the vehicle [3, 4, 5].

The most common types of actuators used in AVSS are electro-hydraulic and electro-pneumatic actuators, but the former are more preferred because of their: superior power-to-weight ratio, fast response, high stiffness, lower cost and lower risk of overheating when used continuously for a long time. However, the effects of actuator dynamics and nonlinearities due to the other suspension elements are often ignored in the published works [3, 5, 6].

Gaspar et al. [7], and Fialho and Balas [8] presented linear parameter varying (LPV) control technique for a nonlinear AVSS with actuator dynamics. LPV theory is mainly useful to tackle measurable and bounded nonlinearities [9]. LPV design is also one of the fixed-gain strategies that are designed to be optimal for nominal parameter set and specific operating condition. Review of other classical, modern and intelligent control techniques that has been applied to AVSS control in the literature is provided in [10].

Model predictive control (MPC) is an iterative, finite horizon optimization control technique. It relies on empirical models obtained by system identification. MPC predicts the outputs based on current plant measurements, set-points of controllers and the modelled dynamic system. While many MPC schemes have been developed; MPC based on the polynomial NARX model is generally desirable because of the plant nonlinearities [11].

Neural network based model predictive control (NN-MPC) has been widely applied in metallurgical processes, chemical plants, food and pharmaceutical processes [12], but the same is not the case for AVSS. This study is motivated by the need for real-time control of AVSS and proper handling of design constraints. The suitability of fuzzy logic and neural network control also arises from their emulation of human logic or brain rather than accuracy of mathematics in modelling nonlinear plants. Fuzzy logic and neural network are therefore useful in by-passing the rigours of directly developing the required dynamic model [4, 13].

NN have found wide applications in the field of system identification and control because of its: ability to ap-

*This paper is an extended version of a paper presented at the IEEE AFRICON 2009 on Sept 23rd, 2009 in Nairobi, Kenya.

O.A. Dahunsi and J.O. Pedro are with School of Mechanical, Industrial and Aeronautical Engineering, University of the Witwatersrand, Johannesburg, South Africa. e-mail: Olurotimi.Dahunsi@students.wits.ac.za and Jimoh.Pedro@wits.ac.za).

proximate arbitrary nonlinear mapping; highly parallel structure which allows parallel implementation, thereby making it more fault-tolerant than conventional schemes; ability to learn and adapt on-line; and good application for multivariable systems [14, 15, 16, 17].

NN model may also be easier to develop than a polynomial AutoRegressive model with eXogenous input (ARX model), especially when applied to multivariable systems. Hence, MPC is often used with other techniques like neural network when dealing with highly nonlinear control applications [18]. NN MPC involves the generation of values for plant inputs as solutions of an online optimization problem. This is done based on prediction of the future plant performance through a NN model obtained for the nonlinear plant [19].

NNAPC uses an indirect design approach by applying the instantaneous linearization principle, this makes approximate predictive control (APC) to be less computationally demanding in comparison to other predictive control methods like the nonlinear predictive control (NPC) and generalized predictive control (GPC). NNAPC can be readily tuned intuitively. It is good for systems with time delay and it is flexible, thus it is effective in a wide spectrum of control applications [11, 20].

Renn and Wu [21] showed that the body displacement responses of a PID controlled nonlinear, quarter-car model compared well with a NN controlled one. However, the NN-based control clearly suppressed the vehicle body acceleration better. Eski and Yildirim [17] compared the suspension deflection response of a linear, full-car AVSS with PID control to a NN MPC of the same AVSS model. Good profile tracking was achieved. Actuator dynamics and system nonlinearities were ignored.

A thorough review of the intelligent control methodologies for AVSS has been presented in [14], this includes adaptive fuzzy, adaptive fuzzy sliding mode, adaptive neural network and GA-based adaptive control. Good performance has been achieved through the application of optimal and robust control to linear AVSS. However, the presence of nonlinearities and uncertainties in the vehicle model calls for better robustness to cater for the multi-objective problem [4, 22, 23]. This situation makes it necessary to either base the AVSS controller design on a combination of modern and intelligent control techniques or solely on intelligent control techniques.

A good vehicle suspension is characterized by good ride comfort, road handling, and road holding qualities within acceptable range of suspension travel [24, 25]. Suspension travel is a readily measurable signal, whose analysis makes the AVSS design realistic [26, 27].

PID controllers are the most widely used controllers for industrial applications, due to their simple structure and the success of Ziegler-Nichols tuning algorithm

[28, 29, 30]. However, tuning of the controller constant gains is often done intuitively and its major disadvantages are in terms of robustness and high loop gains [31]. This motivates for the augmentation of the PID control with evolutionary algorithms (EA) like genetic algorithm (GA) and particle swarm optimization (PSO). These combinations and others, like the combination of PID and Fuzzy control have been reported in literature [4, 30, 32]. PID control is in this work used to benchmark the NNAPC control.

In this paper, NNAPC is proposed for the suspension travel control of an electro-hydraulically actuated vehicle suspension system in the presence of a deterministic road disturbance. The novelty of the paper lies in the application of the designed controller to improve the ride comfort and road handling quality of the AVSS; while simultaneously satisfying the suspension travel and control input constraints.

System identification is a requisite for successful application of NNAPC. It enables the inference of an accurate model or characteristics of a dynamic system from its input-output data. Instantaneous linearization is applied by extracting a linear model from the nonlinear neural network model at each sampling time for control process. Model approximation for the passive vehicle suspension system (PVSS) plant was done using Neural Network AutoRegressive with eXogenous input (NNARX) model.

The paper is structured as follows: Physical and mathematical modelling of the AVSS is presented in section 2. System identification and controller design descriptions are presented in section 3, numerical simulation and discussion of results are presented in section 4. Section 5 gives the concluding remarks.

2 System Overview and Modelling

2.1 Physical Modelling

Figure 1 shows the quarter-car AVSS model, where m_s is the sprung mass, m_u is the unsprung mass, k_s is the suspension spring constant, b_s is the suspension damping coefficient, and k_t is the wheel spring constant. The vertical displacement of the car body, wheel and the road disturbance are represented by x_1 , x_2 and w respectively. The hydraulic actuator force, F , is applied between the sprung and unsprung masses.

The relative displacement between the vehicle body and the wheel, $(x_2 - x_1)$, represents the suspension travel. The relative displacement between the wheel and the road, $(x_2 - w)$, characterizes the road holding quality.

2.2 Mathematical Modelling

Application of Newton's law to the quarter car model shown in Figure 1 yields the following governing equa-

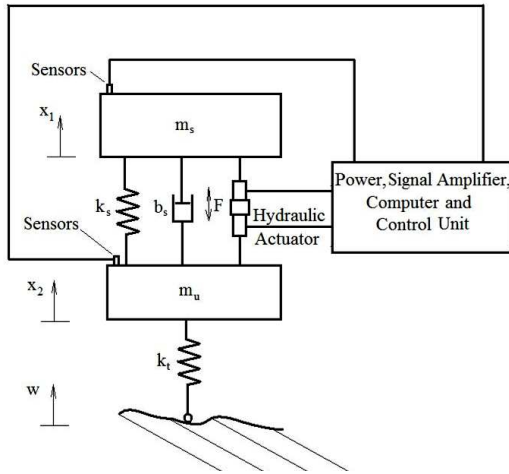


Figure 1: Simplified Quarter Car Model

tions [7, 8]:

$$\begin{aligned} \dot{x}_1 &= x_3 & (1) \\ \dot{x}_2 &= x_4 & (2) \\ m_s \dot{x}_3 &= k_s^l(x_2 - x_1) + k_s^{nl}(x_2 - x_1)^3 \\ &\quad + b_s^l(x_4 - x_3) - b_s^{sym}|x_4 - x_3| \\ &\quad + b_s^{nl}\sqrt{|x_4 - x_3|}sgn(x_4 - x_3) - Ax_5 & (3) \end{aligned}$$

$$\begin{aligned} m_u \dot{x}_4 &= -k_s^l(x_2 - x_1) - k_s^{nl}(x_2 - x_1)^3 \\ &\quad - b_s^l(x_4 - x_3) + b_s^{sym}|x_4 - x_3| \\ &\quad - b_s^{nl}\sqrt{|x_4 - x_3|}sgn(x_4 - x_3) \\ &\quad - k_t(x_2 - w) + Ax_5 & (4) \end{aligned}$$

$$\dot{x}_5 = \gamma\Phi x_6 - \beta x_5 + \alpha A(x_3 - x_4) \quad (5)$$

$$\dot{x}_6 = \frac{1}{\tau}(-x_6 + u) \quad (6)$$

where; $\Phi = \phi_1\phi_2$, $\phi_1 = sgn[P_s - sgn(x_6)x_5]$, $\phi_2 = \sqrt{|P_s - sgn(x_6)x_5|}$, $\alpha = \frac{4\beta_e}{V_t}$, $\beta = \alpha C_{tp}$,

and $\gamma = C_d S \sqrt{\frac{1}{\rho}}$. A is the area of the piston, x_3 and x_4 are vertical velocities of the sprung and unsprung masses respectively, x_5 is the pressure drop across the piston, x_6 is the servo valve displacement, P_s and P_r are the supply and return pressures going into the spool valve, P_u and P_l are the oil pressures in the upper and lower portion of the cylinder. V_t is the total actuator volume, β_e is the effective bulk modulus of the system, Φ is the hydraulic load flow, C_{tp} is the total leakage coefficient of the piston, C_d is the discharge coefficient, S is the spool valve area gradient and ρ is the hydraulic fluid density.

The spring and damping forces have linear and nonlinear components. Spring constant k_s^l and damping coefficient b_s^l affect the spring force and damping force in linear manner. b_s^{sym} contributes an asymmetric characteristics to the overall behaviour of the damper. k_s^{nl} and b_s^{nl} are responsible for the nonlinear components of the spring and damper forces respectively.

Figure 2 illustrates the hydraulic actuator, which is

mounted in between the sprung and the unsprung masses. The actuator is controlled by means of the

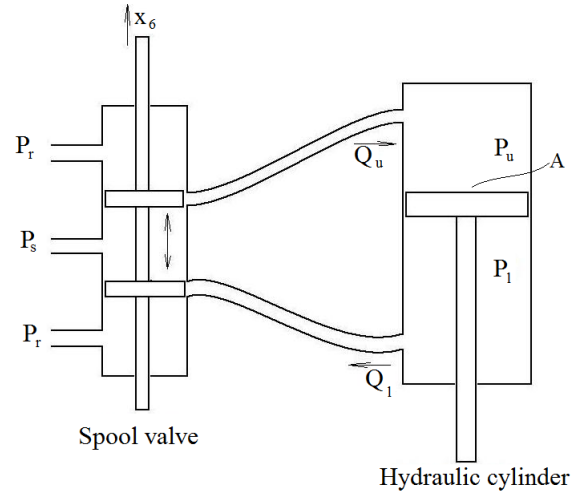


Figure 2: Schematic of the Double Acting Electro-hydraulic Actuator

electro-hydraulic servo-valve in a three-land, four-way spool valve system. The maximum control input (voltage) of 10V was applied to the servo-valves to achieve a maximum suspension travel of ± 10 cm.

It is assumed that the vehicle experiences a sudden bump with amplitude of 11cm, whose profile is shown in Fig. 3 and described by:

$$w(t) = \begin{cases} \frac{a}{2}(1 - \cos\frac{2\pi Vt}{\lambda}) & 1.25 \leq t \leq 1.5 \\ 0 & \text{otherwise} \end{cases} \quad (7)$$

where a is the bump height, V is the vehicle speed and λ is the half wavelength of the sinusoidal road undulation. The values of the system parameters are given in Table 1.

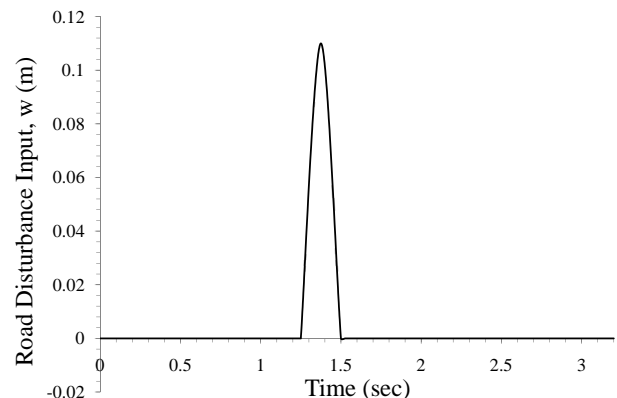


Figure 3: Road Profile

Table 1: Parameters of the Quarter-Car Model [7, 8]

Parameters	Value
Sprung mass (m_s)	290kg
Unsprung mass (m_u)	40kg
Linear suspension stiffness (k_s^l)	$2.35 * 10^4 N/m$
Nonlinear Suspension stiffness (k_s^{nl})	$2.35 * 10^6 N/m$
Tyre stiffness (k_t)	$1.9 * 10^5 N/m$
Linear damping (b_s^l)	$700 Ns/m$
nonlinear damping (b_s^{nl})	$400 Ns/m$
Asymetry damping (b_s^{sym})	$400 Ns/m$
Actuator parameter (α)	$4.515 * 10^{13}$
Actuator parameter (β)	1
Actuator parameter (γ)	$1.545 * 10^9$
Piston area (A)	$3.35 * 10^{-4} m^2$
Supply pressure (P_s)	10,342,500Pa
Actuator time constant (τ)	$3.33 * 10^{-2}$
Amplitude of bump (a)	11cm
Vehicle speed (V)	$30 m.s^{-1}$
Disturbance half wavelength (λ)	7.5m

3 Controller Design

The main performance requirement for the controller is for the AVSS to track a generated desired suspension travel in the presence of a deterministic road disturbance (Eq.(7)). Other performance requirements include [6, 20]:

1. nominal stability,
2. good command tracking,
3. disturbance rejection,
4. rise time not greater than 0.1sec, and
5. maximum overshoot not greater than 5%.

3.1 NN Plant Model Identification

A feedforward, multilayer perceptron (MLP), error back propagation NN was used for the system identification. Training inputs are supplied to the input layer of the network in a forward sweep such that the output of each element is computed layer by layer [33].

Two steps are generally involved in most neural network architectures used for control: system identification and control design. The system identification results in the development of a dynamic model of the plant.

The output of the final layer is compared with the desired output such that the error is back-propagated through the previous layers. The objective of the identification process is to minimize the error signal $\varepsilon(k) = y(k) - \hat{y}(k)$ when the plant and NN model are subjected to the same

input, $u(k)$ (see Figure 4), where $\hat{y}(k)$ is the NN model output, $y(k)$ is the plant output, $y_u(k)$ the true system output, $e(k)$ is noise, $\varepsilon(k)$ is the model residual, θ is the vector of adjustable weights and MSE represents mean squared error which is the performance criterion for the identification process [34].

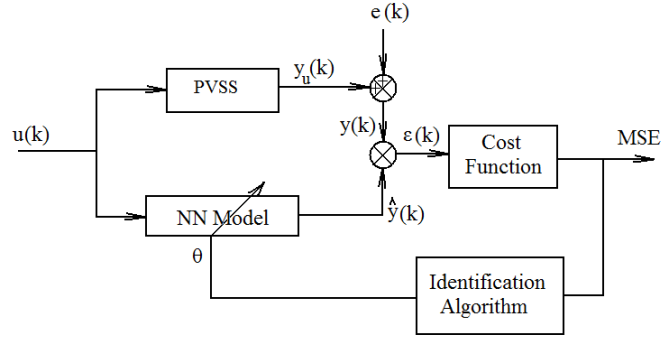


Figure 4: General Structure of System Identification

The identification process consists of four steps: experimentation, model structure selection, model estimation and model validation [11]. Control design stage comes after the system identification, here the NN plant model is used to design the controller.

3.1.1 Experimentation

The PVSS is first identified from a set of input-output data pairs collected from numerical experiments using the PVSS model (Eq.(1)-(6)). The input-output data is collected as shown in Figure 5:

$$Z^N = f[u(k), y(k)]; \quad k = 1, \dots, N \quad (8)$$

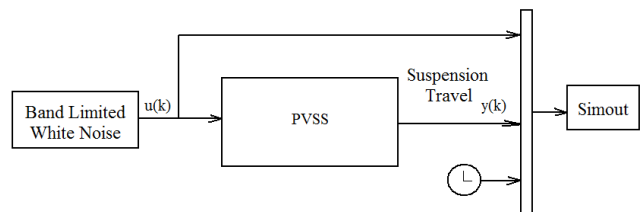


Figure 5: Structure for Input-Output Data Collection

where k is the sampling instant and N is the total number of samples. The sampling time was chosen in accordance with the fastest dynamics of the system which is equivalent to sampling at 1KHz.

The PVSS model identification was conducted using a 20,000 input-output data pairs - split into 10,000 each for training and validation. A non saturating "band-limited white noise" random input was used to excite the PVSS in its operating range, $u(k) \in [-10V, +10V]$.

The estimation and validation data sets are presented in Figures 6 and 7. As part of the data preparation procedure, the data collected were scaled to zero mean and variance 1 before training to enhance faster convergence and improve numerical stability [11].

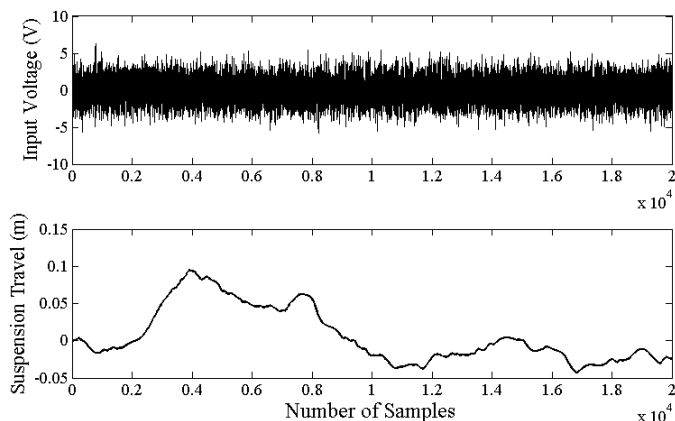


Figure 6: A Snapshot of the Training Data

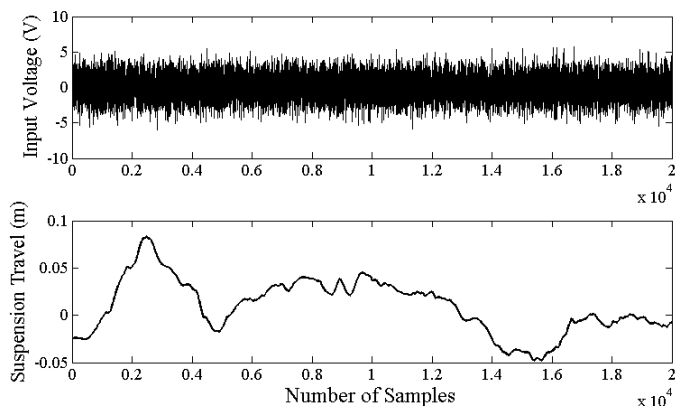


Figure 7: A Snapshot of the Validation Data

3.1.2 Model Structure Selection

NNARX is widely used in representing nonlinear, discrete and time-invariant system. It is simpler, non-recursive (that is, unlike nonlinear models based output error (OE) and Auto Regressive with eXogenous inputs (ARMAX), and more stable since it requires no feedback [11, 35]. The general structure of the NNARX is shown in Figure 8.

Figure 9 shows two stages of NNARX implementation. The regressors are first computed, then a nonlinearity estimator block that consists of a combination of nonlinear and linear functions maps the regressor.

The AVSS nonlinear system is represented by the

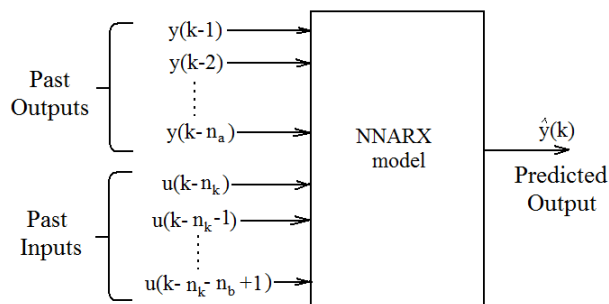


Figure 8: NNARX Model Structure

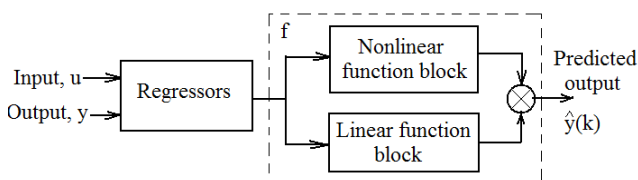


Figure 9: Neural Network Nonlinear ARX Structure

NNARX model structure for a finite number of past inputs $u(k)$ and outputs $y(k)$ [36, 37, 38]:

$$y(k) = f[\phi(k), \theta] + \varepsilon(k) \quad (9)$$

where f is the nonlinear function that is realized by the neural network model, $\phi(k)$ represents the regressors, vector θ contains the adjustable weights and ε represent the model residual.

As a result of the numerical experiment and training, the network implements an estimation of the non-linear transformation, $\hat{f}(\ast)$ which leads to the predicted output. The one-step ahead prediction (1-SAP) based on the identification structure is given by:

$$\hat{y}(k) = f[\phi(k), \theta] \quad (10)$$

and the regression vector is

$$\phi(k) = [y(k-1), y(k-2), \dots, y(k-n_a), u(k-n_k), u(k-n_k-1), \dots, u(k-n_k-n_b+1)]$$

where n_k delay from input to the output in terms of number of samples, while n_a and n_b are the number of past outputs and inputs.

Lipshitz algorithm was used in the determination of the system order. Figure 10 presents the plot of the order index based on the evaluated Lipshitz quotients for the input - output pair combinations against the lag space (number of past inputs and outputs) ranging from 1 to 10.

The slope of the graph can be seen to decrease when the

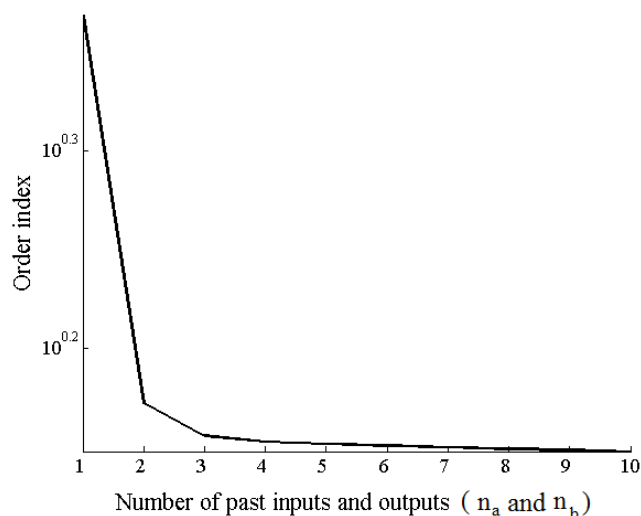


Figure 10: Two Dimensional View of the Order of Index versus Lag Space

model order is ≥ 2 thus defining the "knee point" of the curve and consequently a NNARX model of the order ≥ 2 . This implies that the appropriate number of past inputs and outputs is 2. The number of neurons in the hidden layer becomes five since the hidden layer neuron equals the sum of n_a , n_b and n_k [11, 36]. The choice of a model order that is higher than two may result in lower mean squared error (MSE), but with data overfitting.

3.1.3 Model Estimation

The choice of the the feedforward multi-layer perceptron neural network (MLPNN) structure with backpropagation training for this work is based on its simplicity and computational ease. The two-layer MLPNN structure used is shown in Figure 11. It consists of an input layer that contains two neurons and a bias, while the hidden layer contains five neurons with tangent hyperbolic activation function:

$$f(x) = \tanh(x) = \frac{e^x - e^{-x}}{e^x + e^{-x}}. \quad (11)$$

The output layer contains one neuron with linear activation function [11, 19, 39].

Backpropagation training is a process of training the network with the input and target vectors until it can approximate the desired function, or when it can associate input vectors with appropriate output vectors [33]. During identification, the NN weights are adjusted until its output satisfies the desired MSE performance criteria given as [33, 40]:

$$MSE = \frac{1}{2N} \sum_{k=1}^N [y(k) - \hat{y}(k)]^2 \quad (12)$$

Several backpropagation training algorithms were consid-

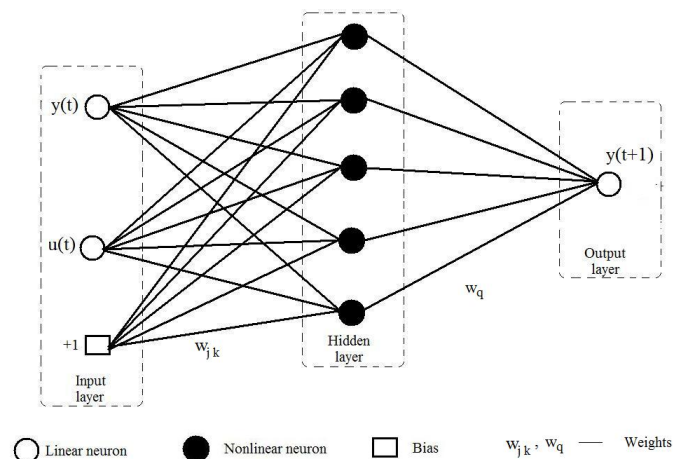


Figure 11: Neural Network Structure

ered for use in training the MLPNN before the Levenberg-Marquardt optimization algorithm was chosen. Table 2 shows the number of epochs and MSE for the tested training algorithms.

Levenberg-Marquardt minimization algorithm is the preferred training algorithm because it improves over time relative to the other algorithms. It is a compromise between the gradient descent and Newton optimization methods. It is a robust algorithm and converges relatively faster [11, 33, 41]. The training parameters for the identification are listed in Table 3.

3.1.4 Model Validation

A MSE performance value of $1.1938e^{-10}$ was attained for the the Levenberg-Marquardt training algorithm at the maximum number of epochs (500) (see Figure 12).

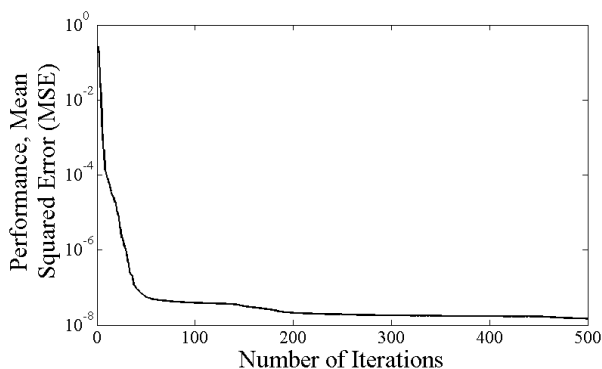


Figure 12: Training of the Plant NN Model.

The one-step ahead prediction and the prediction error plots for the training and validation data are presented in Figures 13 and 14. The one-step ahead prediction data overlapped the training and validation data almost perfectly. This fitness is corroborated by the 10^{-6} and 10^{-5} orders of the residuals for both data.

Table 2: Performance Analysis of Selected Training Algorithms

	Training Algorithm	Full Name of Algorithm	Number of Epochs	MSE
1	trainbfg	Broyden-Fletcher-Goldfarb-Shanno (BFGS) quasi-Newton backpropagation	104	$1.9192 * 10^{-6}$
2	traincgb	Powell-Beale conjugate gradient backpropagation	6	$3.3761 * 10^{-4}$
3	traincgf	Fletcher-Powell conjugate gradient backpropagation	71	$2.7807 * 10^{-6}$
4	traincgp	Polak-Ribiere conjugate gradient backpropagation	74	$3.1559 * 10^{-6}$
5	traingd	Gradient descent backpropagation	500	$4.2644 * 10^{-3}$
6	traingdm	Gradient descent with momentum backpropagation	500	$3.205 * 10^{-3}$
7	traingda	Gradient descent with adaptive learning backpropagation	135	$1.0632 * 10^{-3}$
8	traingdx	Gradient with momentum and adaptive learning backpropagation	213	$1.1512 * 10^{-4}$
9	trainlm	Levenberg-Marquardt backpropagation	500	$1.1938 * 10^{-10}$
10	trainoss	One step secant backpropagation	147	$1.8989 * 10^{-5}$
11	trainrp	Resilient backpropagation	500	$9.6591 * 10^{-7}$
12	trainscg	Scaled conjugate gradient backpropagation	125	$1.0600 * 10^{-5}$

The distribution of the predicted errors is also presented in Figure 15. Although the distribution is skewed to the right in the residuals for validation, the magnitude is too little to make much impact.

However the magnitude of the sampling frequency is high enough to ensure that fitness of the one-step ahead prediction to the measured data is close to 100%, therefore the model validation cannot be based on visual inspection of the fitness one-step ahead prediction with the measured data [11, 36, 34]. Figure 16 shows the cross correlation of the training and validation data. The two plots are similar in the sense that, the latter 60% of both plots falls within the 95% confidence interval.

Table 3: Parameters for the Neural Network Model

Parameters	Value
Total number of samples	20000
Total sampling time	5sec
Maximum number of epochs	500
Sampling frequency	1KHz
Time delay, n_k	1
Training algorithm	Levenberg-Marquandt algorithm
Number of hidden layer neurons	5
Number of past outputs, n_a	2
Number past inputs, n_b	2

3.2 NN-based Approximate Predictive Control (NNAPC)

The control structure in Figure 17 presents an arrangement that allows for selection between the implementation of PID or NNAPC. The NNAPC employs the use of a nonlinear NN plant model to predict future plant responses over a specific period. These predictions subsequently undergo numerical optimisation in a sub-loop to minimise the cost function online.

The NNAPC also involves an optimisation process which is realised through the minimization of the cost function [11, 39]:

$$J(t, U(t)) = \sum_{i=N_1}^{N_2} [r(t+i) - \hat{y}(t+i)]^2 + \rho \sum_{i=1}^{N_u} [\Delta u(t+i-1)]^2 \quad (13)$$

the future controls are given by

$$U(t) = [u(t) \dots u(t+N_u-1)]^T$$

and subjected to the constraint given by

$$\Delta u(t+i) = 0, \quad N_u \leq i \leq N_2 - d$$

the tuning parameters are; N_1 - minimum prediction horizon or minimum cost, it is equal to the time delay of the system in this case. N_2 - maximum control horizon, ρ - the weighting factor penalizing changes in the control

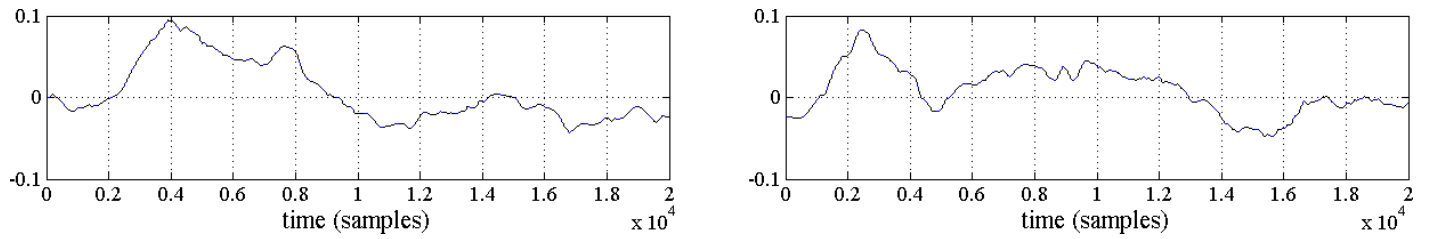


Figure 13: One-Step Ahead Prediction Fitness with the Training and Validation Data

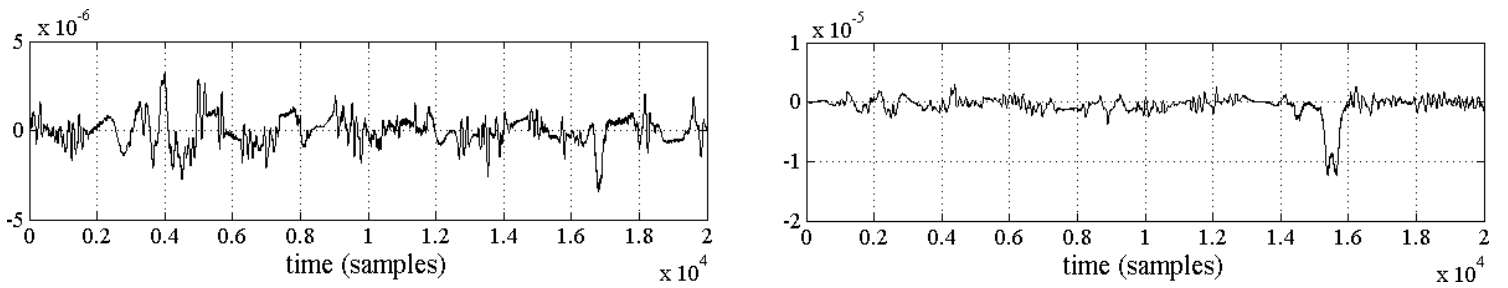


Figure 14: Prediction Error for the Training and Validation Data

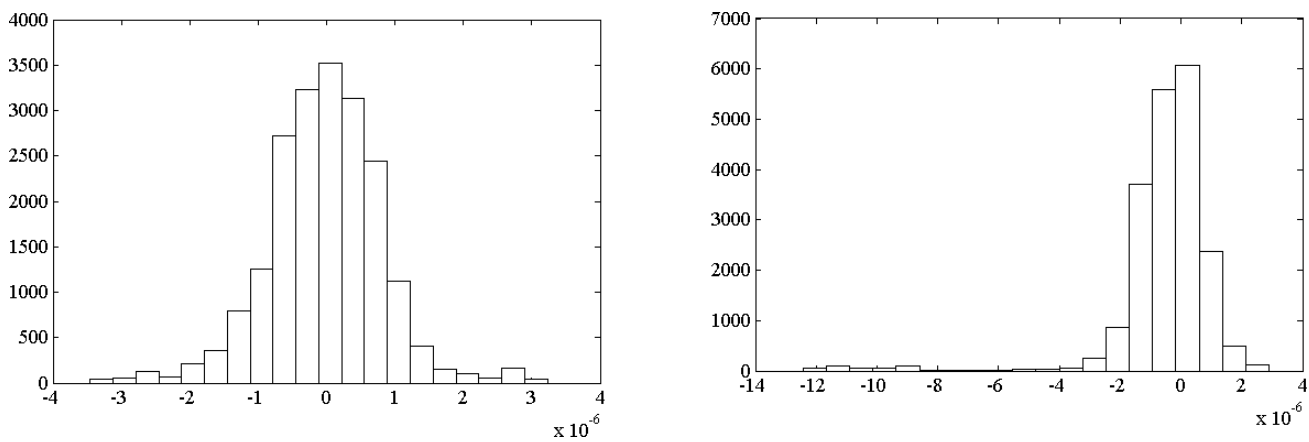


Figure 15: Histograms of Prediction Errors for the Training and Validation Data

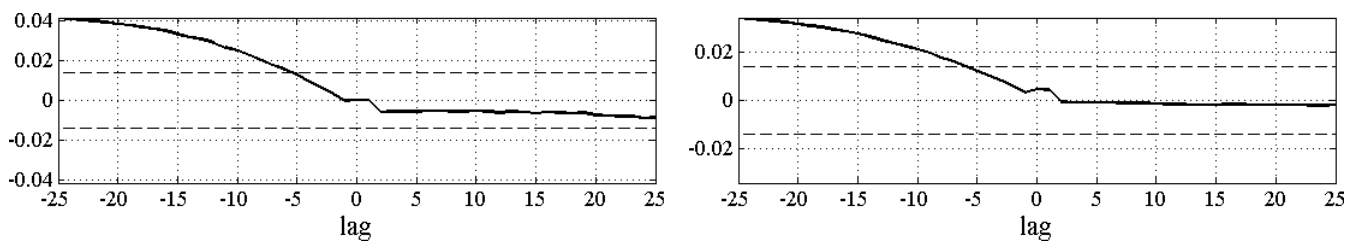


Figure 16: Cross-Correlation of the Training and Validation Data

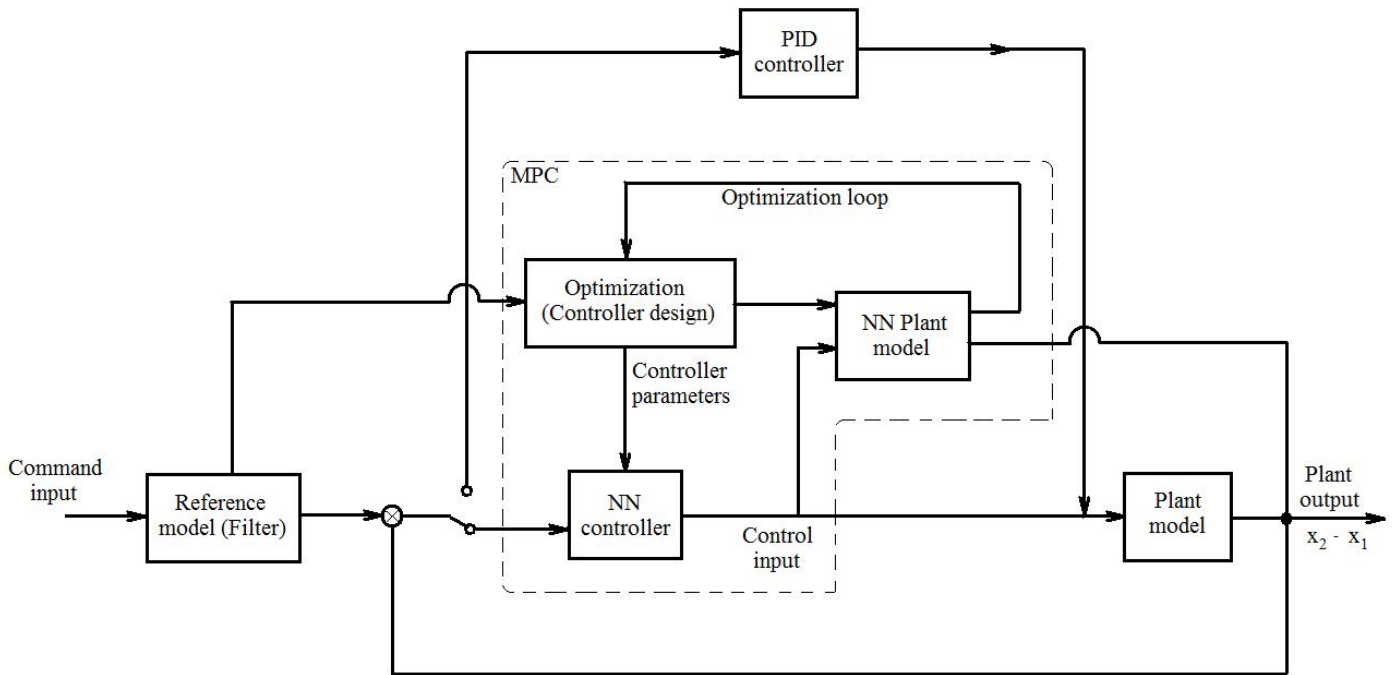


Figure 17: Architecture for PID and NN based APC

input, T_s is the sampling time and the total number of sample was 500. A variable but preset control input in the form of voltage (which was ≤ 10 volts) was supplied to the servo-valve to generate the actuation force at the piston. The NNAPC and PID controller's parameters used for the simulations are given in Table 4

Table 4: NNAPC and PID tuning parameters

NNAPC		PID Tuning	
Parameters	Value	Parameters	Value
N_1	1	K_p	3.0
N_2	8	T_i	15
N_u	1	T_d	0.04035
ρ	0.03	α	0.047

3.3 PID Control and Tuning

The structure of the PID controller is given as [39, 42]:

$$U(s) = \left(K_p \frac{1 + T_i s}{T_i s} \frac{1 + T_d s}{1 + \alpha T_d s} \right) E(s) \quad (14)$$

where $E(s) = Y_{ref}(s) - Y(s)$ is the error signal between the reference signal $Y_{ref}(s)$ and the actual output signal $Y(s)$, $U(s)$ is the plant input signal, K_p is the proportional gain, T_d is the derivative time constant, T_i is the integral time constant and α is the lag factor in the derivative component of the PID controller.

The PID controller was tuned in accordance with the recommendation in [42] for the classical cascade PID controller. Ziegler-Nichols tuning rule is used with a decay ratio of 0.25 to obtain the PID controller gains. This is because PID controllers can easily generate too high control inputs which can lead to saturation.

4 Simulation Results and Discussion

The NNAPC and PID controllers were applied to an AVSS nonlinear model with actuation force generated by an electro-hydraulic actuator. The NN-based identification process was implemented in MATLAB using Levenberg-Marquardt training algorithm.

The AVSS suspension travel responses in Figures 18 and 19 show a good command tracking by both controllers, except at the points where the values of the desired output changes, here both controllers have overshoots.

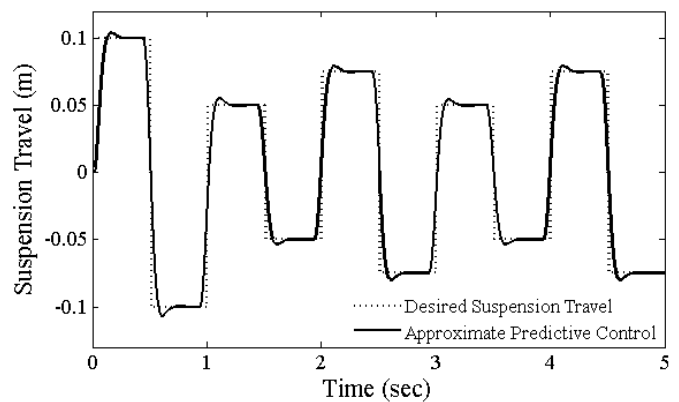


Figure 18: Suspension Travel Tracking for Neural Network based APC

The PID controller has better rise time but with significant overshoots. The rise time for the NNAPC is marginally above the specified value but its overshoots are below the specified value. Both controllers have zero steady state error until the transition points are approached.

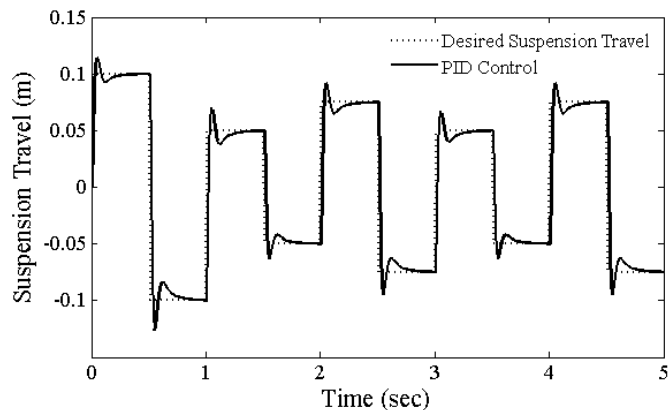


Figure 19: Suspension Travel Tracking for PID Control

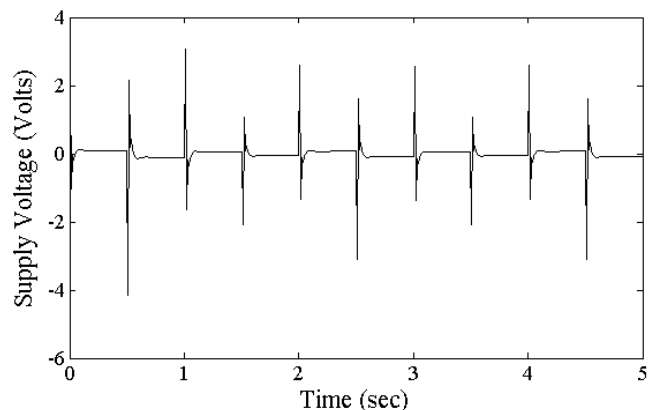


Figure 21: PID Control Input

The PID controller has pronounced overshoots at the transition points. Measured performances of the controllers against specified performance parameters are presented in Table 5.

Table 5: Performance Evaluation

Performance parameters	Specified value	NNAPC	PID
Over-shoot	5%	4.1%	14.1%
Rise Time(sec)	0.1	0.1057	0.0304
Steady state error	0%	0%	0%

Figure 20 shows the control input for the NNAPC. The supplied voltage values range between (approximately) -0.15V and 0.2V. Small voltage spikes are visible at the transition points. Figure 21 shows the control input for

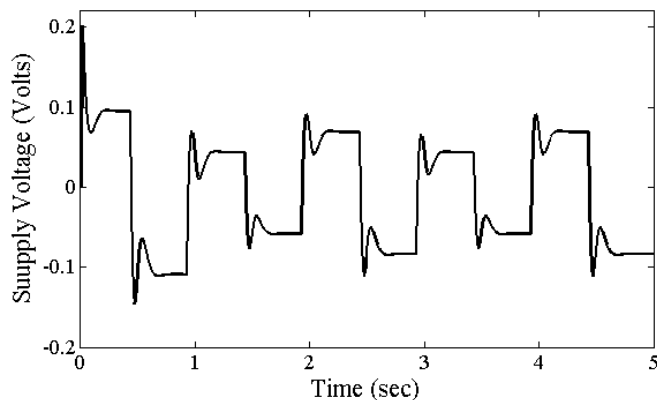


Figure 20: Approximate Predictive Control Input

the PID controller. PID control is achieved at much greater cost, as shown with surges of magnitude ranging from (approximately) -4V to 3V occurring at the transition points.

5 Conclusion

A NNAPC controller has been designed for a nonlinear AVSS. The system identification and control of the AVSS

took into account the effect of the actuator dynamics. The nonlinear system was identified using a two layer MLPNN with five hidden layer neurons and the quality of the neural network model that resulted from the system identification is evident from the model validation analysis and the NNAPC control results.

The designed controller shows better tracking of the desired output in the presence of deterministic disturbance input than the constant-gain PID controller. Although it shows marginal overshoots at the transition points of the desired output being tracked, the optimization module of the NNAPC was able to cut down on the tasking computational works which makes real-time control challenging.

Although it is normally expected that a control system like NNAPC that is based on instantaneous linearization, will only have good performance around or near an operating point, the reference tracking control has demonstrated the flexibility of NNAPC when applied to AVSS.

References

- [1] Hada, M. K., Menon, A. and Bhawe, S.Y., "Optimisation of an Active Suspension Force Controller using Genetic Algorithm for Random Input," *Defence Science Journal*, Vol. 57, No. 5, pp. 691-706, September, 2007.
- [2] He, Y. and McPhee, J., "A Design Methodology for Mechatronic Vehicles: Application of Multidisciplinary Optimization, Multibody Dynamics and Genetic Algorithms," *Vehicle Systems Dynamics*, Vol. 43, No. 10, pp. 697-733, October, 2005.
- [3] Shen, X. and Peng, H., "Analysis of Active Suspension Systems with Hydraulic Actuators," *Proceedings of the 2003 IAVSD Conference*, Atsuigi, Japan, pp. 1-10, August, 2003.
- [4] Feng, J. Z., Li, J., Li and F. Yu", "GA-Based PID and Fuzzy Logic Control for Active Vehicle Suspension System," *International Journal of Automotive*

- Technology*, Vol. 4, No. 4, pp. 181-191, December, 2003.
- [5] Chantranuwathana, S. and Peng, H., "Adaptive Robust Force Control for Vehicle Active Suspension," *International Journal of Adaptive Control and Signal Processing*, Vol. 18, No. 2, pp. 83-102, March, 2004.
- [6] Pedro, J. O., " H_2 - LQG/LTR Controller Design for Active Suspension Systems," *R and D Journal of the South African Institution of Mechanical Engineering*, Vol. 23, No. 2, pp. 32-41, November, 2007.
- [7] Gaspar, P., Szaszi, I. and J. Bokor, Active Suspension Design Using Linear Parameter Varying Control, *International Journal of Autonomous Systems (IJVAS)*, Vol. 1, No. 2, pp. 206-221, June, 2003.
- [8] Fiahlo, I. and Balas, G. J., "Road Adaptive Active Suspension using Linear Parameter-Varying Gain-Scheduling," *IEEE Transactions on Control Systems Technology*, Vol. 10, No. 1, pp. 43-54, January, 2002.
- [9] Poussot-Vassal, C., Senname, O., Dugard, L., Gaspar, P., Szabo, Z., and Bokor, J., "Multi-objective qLPV H_∞/H_2 Control of a Half Vehicle," *Proceedings of the 10th MINI Conference on Vehicle System Dynamics, Identification and Anomalies*, Budapest, Hungary, 2006.
- [10] Hrovat, D., "Survey of Advanced Suspension Developments and Related Optimal Control Applications," *Automatica*, Vol. 33, No. 10, pp. 1781-1817, October, 1997.
- [11] Norgaard, M., Ravn, O., Poulsen N. K. and Hansen L. K., *Neural Networks for Modelling and Control of Dynamic Systems: A Practitioner's Handbook*, Springer, Boston, MA, 2000.
- [12] J.M.Galvez, J. M., Zarate, L. E. and Helman, H., "A Model-Based Predictive Control Scheme for Steel Rolling Mills Using Neural Networks," *Journal of the Brazilian Society of Mechanical Sciences and Engineering*, Vol. 25, No. 1, pp. 85-89, March, 2003.
- [13] Huang, S. J. and Lin, W. C., "A Neural Network Based Sliding Mode Controller for Active Vehicle Suspension," *Proceedings of the Institute of Mechanical Engineers, Part D*, Vol. 221, No. 11, pp. 1381-1397, November, 2007.
- [14] Cao, J., Liu, H., Li, P. and Brown, D., "State of the Art in Vehicle Active Suspension Adaptive Control Systems based on Intelligent Methodologies," *IEEE Transactions of Intelligent Transportation Systems*, Vol. 9, No. 3, pp. 392-405, September, 2008.
- [15] Al-Holou, N., Lahdhiri, T., Joo, D. S., Weaver, J. and Al-Abbas, F., "Sliding Model Neural Network Inference Fuzzy Logic Control for Active Suspension System," *IEEE Transaction on Fuzzy System*, Vol. 10, No. 2, pp. 234-245, April, 2002.
- [16] Jin, Y. and Yu, D. J., "Adaptive Neuron Control Using an Integrated Error Approach with Application to Active Suspensions," *International Journal of Automotive Technology*, Vol. 9, No. 3, pp. 329-335, June, 2008.
- [17] Eski, I. and Yildirim, S., "Vibration Control of Vehicle Active Suspension System Using a New Robust Neural Network Control System," *Simulation Modelling Practice and Theory*, Vol. 17, No. 5, pp. 778-793, May, 2009.
- [18] Yu, D. L. and Gomm, J. B., "Implementation of Neural Network Predictive Control to a Multivariable Chemical Reactor," *Control Engineering Practice*, Vol. 11, No. 11, pp. 1315-1323, November, 2003.
- [19] Hagan, M. T., Demuth, H. B. and Jesus, O., "An Introduction to the use of Neural Networks in Control Systems," *International Journal of Robust and Non-Linear Control*, Vol. 12, No. 11, pp. 959-985, September, 2002.
- [20] Dahunsi, O. A., Pedro, J. O. and Nyandoro O. T., "Neural Network-Based Model Predictive Control of a servo-Hydraulic Vehicle Suspension System," *Proceedings of the IEEE AFRICON2009 Conference*, Nairobi, Kenya, pp.1-6, September, 2009.
- [21] Renn, J. and Wu, T., "Modelling and Control of a new $\frac{1}{4}T$ Servo-Hydraulic Vehicle Active Suspension System," *Journal of Marine Science and Technology*, Vol. 15, No. 3, pp. 265-272, September, 2007.
- [22] Yoshimura, T. and Temura, I., "Active Suspension Control of a One-Wheel Car Model Using Single Input Rule Modules Fuzzy Reasoning and a Disturbance Observer," *Journal of Zhejiang University Science*, Vol. 6A, No. 4, pp. 251-256, 2005.
- [23] Spentzas, K. N. and Kanarachos, S. A., "A Neural Network Approach to the Design of a Vehicle's Non-Linear Hybrid Suspension System," *Proceedings of the Institute of Mechanical Engineers, Part B*, Vol.216, No. 5, pp. 833-838, May, 2002.
- [24] Du, H. and Zhang, N., " H_∞ Control of Active Vehicle Suspensions with Actuator Time Delay," *Journal of Sound and Vibration*, Vol. 301, No. 1-2, March, 2007.
- [25] Kumar, M. S. and Vijayarangan, S., "Analytical and Experimental Studies on Active Suspension System of Light Passenger Vehicle to Improve Ride Comfort," *Mechanika*, Vol. 65, No. 3, pp. 34-41, June, 2007.

- [26] Gao, B., Tilley, D. G., Williams, R. A., Bean, A. and Donahue, J., "Control of Hydropneumatic Active Suspension based a Non-linear Quarter-Car Model," *Proceedings of the Institute of Mechanical Engineers, Part I*, Vol. 220, No. 1, pp. 31-75, January, 2006.
- [27] Du, H. and Zhang, N., "Designing H_∞/GH_2 Static - Output Feedback Controller for Vehicle Suspensions Using Linear Matrix Inequalities and Genetic Algorithms," *Vehicle Systems Dynamics*, Vol. 46, No. 5, pp. 385-412, May, 2008.
- [28] Juang, J. G., Huang, M. T. and Liu, W. K., "PID Control using Presearched Genetic Algorithm for a MIMO System," *IEEE Transactions on Systems, Man and Cybernetics-Part C : Applications and Reviews*, Vol. 38, No. 5, September, 2008.
- [29] Senthil Kumar, M., "Development of Active Suspension System for Automobiles using PID Controller," *Proceedings of the World Congress on Engineering 2008 Vol II WCE 2008*, London, U.K., July, 2008.
- [30] Iruthayarajan, M. W. and Baskar, S., "Evolutionary Algorithms Based Design of Multivariable PID Controller," *Expert Systems with Applications*, Vol. 36, No. 5, July, 2009.
- [31] Gao, Z., "From Linear to Nonlinear Control Means: A Practical Progression," *ISA Transactions*, Vol. 41, No. 2, pp. 177-189, April, 2002.
- [32] Kuo, Y. and Li, T. S., "GA-Based Fuzzy PI/PD Controller for Automotive Active Suspension System," *IEEE Transactions on Industrial Electronics*, Vol. 46, No. 6, pp. 1051-1056, December, 1999.
- [33] Demuth, H. and Beale, M., "Neural Networks Toolbox Users Guide: For use with MATLAB," The MathWorks, Inc., Natick, Massachusetts, 2002.
- [34] Jelali, M., and Kroll A., *Hydraulic Servo-Systems:Modelling, Identification and Control*, Springer-Verlag, London, 2003.
- [35] K. K. Ahn, H. P. H. Ahn and N. T. Kiet: "A Comparative Study of Modelling and Identification of the Pneumatic Artificial Muscle (PAM) Manipulator based on Recurrent Neural Networks", *Proceedings of the International Symposium on Electrical and Electronics Engineering*, HCM city, Vietnam, 2007.
- [36] N. Kishor, R. P. Saini and S. P. Singh: "Small Hydro Power Plant Identification Using NNARX Structure", *Neural Computing and Applications*, Vol. 14 No. 3, pp. 212 - 222, September 2005.
- [37] Q. Zhang and L. Ljung: "Multiple Steps Prediction with Nonlinear ARX Models", *Proceedings of the Symposium on Nonlinear Control Systems (NOLCOS)*, Stuttgart, Germany, 2004.
- [38] M. H. F. Rahiman, M. N. Taib and Y. M. Salleh: "Selection of Training Data for Modelling Essential Oil Extraction System using NNARX Structure", *Proceedings of the International Conference on Control, Automation and Systems*, Seoul, Korea, 2007.
- [39] Norgaard, M., "Neural Networks Based Control System Design," *Tech.Report 00-E-892*, Department of Automation, Technical University of Denmark, 2000.
- [40] Mjalli, F. S. and Al-Asheh, S., "Neural-Networks-Based Feedback linearization versus Model Predictive Control of Continuous Alcoholic Fermentation Process," *Chemical Engineering Technology*, Vol. 28, No. 10, pp. 1191-1200, October, 2005.
- [41] Haykin, S., "Neural Networks and Learning Machines," Pearson Education, Inc., New Jersey, 2009.
- [42] O'Dwyer, A., "Handbook of PI and PID Controller Tuning Rules," Imperial College Press, London, 2006.